Selenium-bridged diiron hexacarbonyl complexes as biomimetic models for the active site of Fe–Fe hydrogenases†

Shang Gao, Jiangli Fan, Shiguo Sun, Xiaojun Peng,* Xing Zhao and Jun Hou

Received 12th November 2007, Accepted 31st January 2008
First published as an Advance Article on the web 27th February 2008
DOI: 10.1039/b717497g

Three N-substituted selenium-bridged diiron complexes [{(μ-$SeCH_2)_2NC_6H_4R$}$Fe_2(CO)_6$] (R = 4-NO_2, **7**; R = H, **8**; R = 4-CH_3, **9**) were firstly prepared as biomimetic models for the Fe–Fe hydrogenases active site. Models **7–9** could be generated by the convergent reaction of [(μ-$HSe)_2Fe_2(CO)_6$] (**6**) with *N*,*N*-bis(hydroxymethyl)-4-nitroaniline (**1**), *N*,*N*-bis(hydroxymethyl)aniline (**2**), and *N*,*N*-bis(hydroxymethyl)-4-methylaniline (**3**) in 46–52% yields. All the new complexes **7–9** were characterized by IR, ^{1}H and ^{13}C NMR and HRMS spectra and their molecular structures were determined by single-crystal X-ray analysis. The redox properties of **7–9** and their dithiolate analogues [{(μ-$SCH_2)_2NC_6H_4R$}$Fe_2(CO)_6$] (R = 4-NO_2, **7s**; R = H, **8s**; R = 4-CH_3, **9s**) were evaluated by cyclic voltammograms. The electrochemical proton reduction by **9** and **9s** were investigated in the presence of *p*-toluenesulfonic acid (HOTs) to evaluate the influence of changing the coordinating S atoms of the bridging ligands to Se atoms on the electrocatalytic activity for proton reduction.

Introduction

Hydrogen evolution and uptake in nature is mostly catalyzed by the metalloenzymes called hydrogenases.[1] Among these, Fe–Fe hydrogenases (Fe H_2ases) have received more attention than other types of hydrogenases because of their significant efficiency (6000–9000 molecules H_2 s^{-1} per site) in the production of hydrogen.[2,3] Crystallographic and IR spectroscopy studies revealed the active site of Fe H_2ase contains a butterfly 2Fe2S subunit, in which one of the iron atoms is linked to a cuboidal 4Fe4S cluster by a cystenyl-S bridge (Fig. 1).[4] The 4Fe4S unit is actually responsible for the electron transfer while the 2Fe2S subunit is responsible for hydrogen formation and activation. The two iron atoms in the 2Fe2S subunit are decorated by the biologically unusual carbon monoxide and cyanide ligands and are bridged by a three-atoms-containing dithiolate ligand. Very recent crystallographic studies with higher resolution,[5] together with theoretical studies,[6] suggest the bridging dithiolate ligand as azadithiolate (ADT) SCH_2NHCH_2S or the N-substituted species, and the nitrogen heteroatom plays an important role for the heterolytic cleavage or formation of H_2 in the natural system.

The structural elucidation of the active site of the Fe H_2ases led to a renaissance in the chemistry of the well-known transition metal sulfides [(μ-$SR)_2Fe_2(CO)_6$], the structures of which resembled the 2Fe2S subunit of the Fe H_2ases active site, and raised their profile as the potential bioinorganic hydrogen activation catalysts. In this spirit, a great variety of diiron dithiolate complexes have been prepared as the structural and functional models for the Fe H_2ases active site.[7–10] Nevertheless, most of the efforts have been performed on structure modifications by phosphane,[7f–i,11]

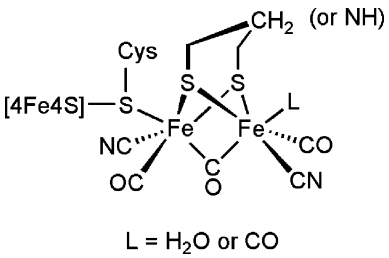

Fig. 1 Structure of the enzyme active site obtained from protein crystallography.

cyanide,[7a–c,10b,12] isocyanide[13] and N-heterocyclic carbene[14] ligands exchange and X atom variation in the dithiolate bridge –SCH_2XCH_2S–.[15] To the best of our knowledge, there have been few reports on the effects of changing the coordinating S atoms of the bridging dithiolate ligands on the biomimetic models,[16,17] and no biomimetic model bearing the –$SeCH_2NRCH_2Se$– bridge with general formula [(μ-$SeCH_2)_2NR$]$Fe_2(CO)_6$] (aza diselenide diiron complexes) has been prepared. With this in mind, we synthesized a series of aza diselenide diiron complexes [{(μ-$SeCH_2)_2NC_6H_4R$}$Fe_2(CO)_6$] (R = 4-NO_2, **7**; R = H, **8**; R = 4-CH_3, **9**) (Scheme 1), in which the S atoms in [{(μ-$SCH_2)_2NR$}$Fe_2(CO)_6$] species were substituted with Se atoms. Se atoms were introduced for the purposes: (i) the architectures of the diselenide diiron complexes should be similar to those of their dithiolate analogues without complicating the element group from sulfur to selenium; (ii) the Se atoms should have influence on the reactivity and the redox properties of the iron cores for their different electronic properties as compared to S atoms. The attaching of a series of aromatic rings with different inductive effects to the bridging nitrogen atom would provide us an insight into the common influence of Se atoms on the biomimetic models for the Fe H_2ase active site. Herein, we describe the preparation, the spectroscopic and the structural characterization of the three aza diselenide diiron complexes **7–9**, as well as the redox properties of **7–9**

State Key Laboratory of Fine Chemicals, Dalian University of Technology, Zhongshan Road 158-40, Dalian, 116012, PR China. E-mail: pengxj@dlut.edu.cn; Fax: +86 411/88993906; Tel: +86 411/88993899

† CCDC reference numbers 665465–665467. For crystallographic data in CIF or other electronic format see DOI: 10.1039/b717497g

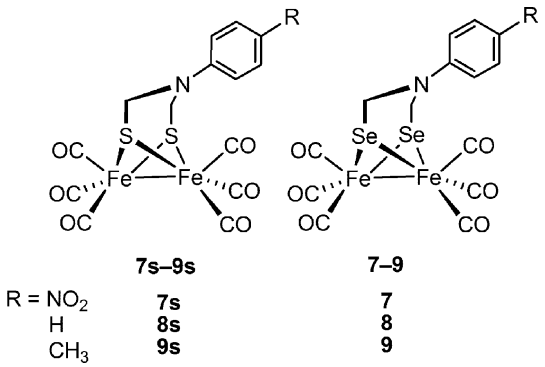

Scheme 1 The prepared aza diselenide diiron complexes **7–9** and their dithiolate analogues **7s–9s**.

and their dithiolate analogues [{(μ-SCH_2)$_2$$NC_6H_4R$}$Fe_2(CO)_6$] (R = 4-$NO_2$, **7s**; R = H, **8s**; R = 4-CH_3, **9s**) (Scheme 1). The electrochemical response of **9** and **9s** in the presence of *p*-toluenesulfonic acid (HOTs) indicate that **9** has a slightly greater electrocatalytic activity for proton reduction as compared to **9s**.

Results and discussion

Synthesis and spectroscopic characterization of complexes 7–9

The synthetic methods for the target complexes **7–9** are somewhat different from those of their dithiolate analogues **7s–9s**[9a,c,13c] (Scheme 2). The *N*,*N*-bis(hydroxymethyl)amines $RC_6H_4N(CH_2OH)_2$ (R = 4-NO_2, **1**; R = H, **2**; R = 4-CH_3, **3**) were readily accessible from the reaction of the primary amines (4-nitroaniline, aniline, 4-methylaniline) with paraformaldehyde in the methanol solution of KOH. This method was improved from literature[18] and the additional KOH made the paraformaldehyde dissolved completely in methanol. The homogeneous reaction took place immediately and completely after 4–5 hours. The precursors **1–3** could be generated according *ca.* 80–90% yield. Although **1–3** could be prepared by the heterogeneous procedure in which the primary amines directly reacted with the paraformaldehyde in CH_2Cl_2,[10a] the yields were very low. To avoid using the insalubrious reagent $SOCl_2$, the halogenation of **1–3** was not used but the hydroxymethylamines were used directly in the next step without isolation.

Another precursor [(μ-Se)$_2$$Fe_2(CO)_6$] (**4**) could be obtained according to literature methods.[19,20] **4** could be purified by column chromatography using hexane as eluant and its structure was analogous to [(μ-S)$_2$$Fe_2(CO)_6$].[21] It is noteworthy that **4** decomposes rapidly in the solid state while in solution it can be stored at 0 °C for several days. Treat the freshly prepared THF solution of **4** with $LiEt_3BH$, a reagent known to cleave Se–Se bond,[22] at −78 °C generated the lithium salt of hexacarbonyldiselenidediiron (**5**).[19,23] After the subsequent protonation of **5** with CF_3COOH, the resulting [(μ-HSe)$_2$$Fe_2(CO)_6$] (**6**) reacted with precursors **1–3** to give the corresponding aza diselenide diiron complexes **7–9** in moderate yields. Unlike their precursor **4**, complexes **7–9** are stable to air in the solid state but moderately sensitive in solution.

Complexes **7–9** were characterized by ^{1}H and ^{13}C NMR, IR and mass spectrometry. The results of the HR-MS analyses for the three complexes are all in good agreement with the supposed molecular weight. The absorption for the terminal carbonyls of **7–9** are listed in Table 1 together with their dithiolate analogues **7s–9s** for comparison. All complexes show three strong bands in the carbonyl region of 1983–2078 cm^{-1}. The average *ν*(CO) values of **7–9** are shifted towards lower frequencies with respect to those of their dithiolate analogues **7s–9s** by 8, 9 and 11 cm^{-1},

Table 1 A comparison of *ν*(CO) bands of **7–9** and their dithiolate analogues **7s–9s**[a]

Complex	*ν*(CO)/cm^{-1}	Average value of *ν*(CO)/cm^{-1}
7	2070, 2033, 1999	2034
8	2067, 2030, 1994	2030
9	2064, 2023, 1983	2023
7s	2078, 2040, 2008	2042
8s	2076, 2038, 2002	2039
9s	2071, 2030, 2000	2034

[a] IR spectra were measured in CH_2Cl_2.

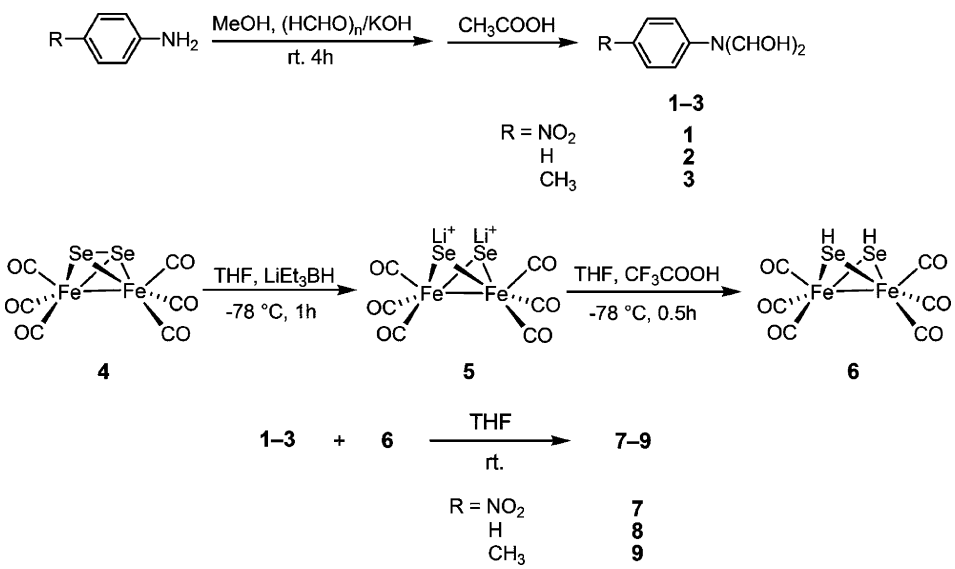

Scheme 2 The synthetic procedure of complexes **7–9**.

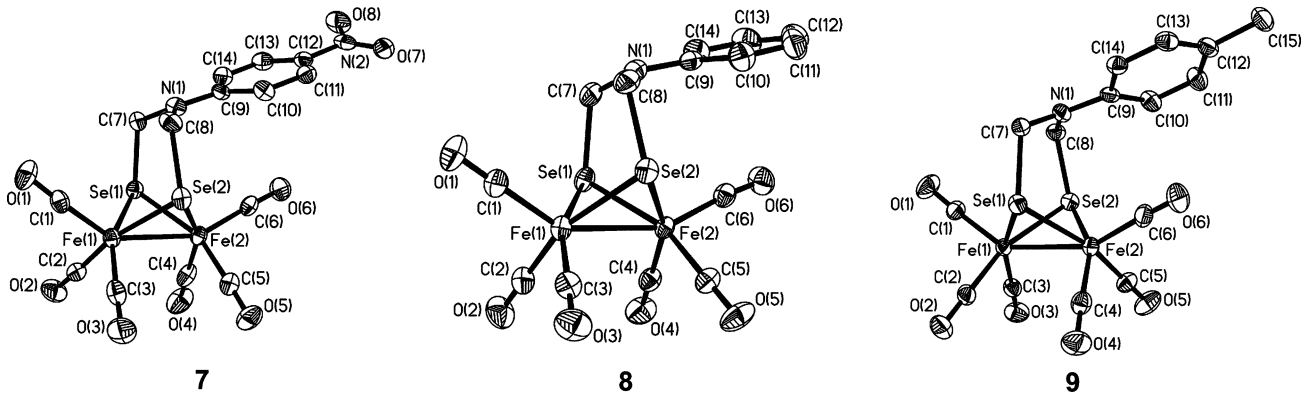

Fig. 2 ORTEP views of **7**, **8** and **9** with 30% probability level ellipsoids.

respectively, which indicates a slight enhancement of the electron density at the iron cores for **7–9**. Such variation is attributed to the better electron-donating capability of Se atoms which results in the higher electron density of the iron cores. Consequently, the enhanced feedback bonds from Fe atoms to CO cause the red-shifts of the ν(CO) frequencies of **7–9**.

Molecular structures of complexes 7–9

The molecular structures of **7–9** were confirmed by single-crystal X-ray analysis. While ORTEP diagrams of **7–9** are shown in Fig. 2, the selected bond lengths and angles are listed in Table 2. As expected, the overall molecular geometries of **7–9** are analogous to those of their dithiolate analogues **7s–9s**[9a,c,13c] and other previously reported aza dithiolate diiron derivatives.[9,24]

The 2Fe2Se cores of all three complexes adopt a butterfly framework. Each iron atom is coordinated to three terminal carbonyl ligands in a distorted square-pyramidal geometry. Complexes **7–9** each contains two fused six-membered rings which are formed by their two iron atoms and the N-substituted aza diselenide bridge. The *p*-substituted phenyl moiety attached to the bridged nitrogen atom lies in an equatorial position relative to the metalloheterocycle for the all three complexes and slants towards the Fe(2)$(CO)_3$ unit. The long-range interaction between the arene group and the closest Fe$(CO)_3$ unit impacts the C–Fe–Fe angle. Thus, compared with the C(1)–Fe(1)–Fe(2) angle, C(6)–Fe(2)–Fe(1) angle was enlarged by 7.49° for **7**, 7.64° for **8** and 6.89° for **9**, respectively. The nitrogen long pair of **7–9** resides in an axial position and the sum of the C–N–C angles around the N atom is 357.6° for **7**, 355.4° for **8** and 357.5° for **9**. These sum values agree well with those of **7s–9s** (357.7° for **7s**, 355.0° for **8s** and 357.4° for **9s**)[9a,c,13c] and imply that the sp^2-hybridized N atom slightly deviates from the plane defined by the N(1), C(7), C(8) and C(9) atoms (for **7–9**) and the p–π conjugation between the substituted phenyl ring and the p-orbital of the bridged N atom is somewhat weakened.

Table 2 Selected bond lengths (Å) and angles (°) for complexes **7–9**

	7	8	9
Fe(1)–Fe(2)	2.5475(10)	2.5572(5)	2.5514(9)
Fe(1)–Se(1)	2.3676(8)	2.3903(5)	2.3790(8)
Fe(1)–Se(2)	2.3870(8)	2.3791(4)	2.3811(9)
Fe(2)–Se(1)	2.3756(9)	2.3703(4)	2.3792(9)
Fe(2)–Se(2)	2.3850(8)	2.3840(4)	2.3772(9)
Se(1)–C(7)	1.990(5)	2.010(3)	2.018(4)
Se(2)–C(8)	2.013(5)	2.021(3)	2.002(4)
N(1)–C(7)	1.430(6)	1.426(4)	1.427(5)
N(1)–C(8)	1.429(6)	1.407(4)	1.420(5)
N(1)–C(9)	1.403(6)	1.408(4)	1.407(5)
Se(1)···Se(2)	3.2704(7)	3.2637(4)	3.2718(8)
C(1)–Fe(1)–Fe(2)	145.95(17)	147.72(10)	145.32(14)
C(6)–Fe(2)–Fe(1)	153.44(17)	155.36(8)	152.21(15)
Fe(1)–Se(1)–Fe(2)	64.97(3)	64.979(13)	64.85(3)
Fe(1)–Se(2)–Fe(2)	64.53(3)	64.943(13)	64.85(2)
Se(1)–Fe(1)–Se(2)	86.92(3)	86.359(15)	86.84(3)
Se(1)–Fe(2)–Se(2)	86.78(3)	86.703(13)	86.92(2)
C(7)–Se(1)–Fe(1)	107.89(17)	110.08(11)	108.45(13)
C(8)–Se(2)–Fe(1)	106.15(16)	104.58(9)	105.82(13)
C(7)–Se(1)–Fe(2)	111.68(16)	110.27(7)	110.35(11)
C(8)–Se(2)–Fe(2)	111.21(14)	110.94(9)	111.12(12)
C(1)–Fe(1)–Se(1)	101.61(19)	103.03(9)	100.43(13)
C(1)–Fe(1)–Se(2)	97.86(15)	99.38(9)	98.36(15)
C(6)–Fe(2)–Se(1)	102.74(19)	104.56(8)	98.37(14)
C(6)–Fe(2)–Se(2)	107.79(16)	108.18(8)	112.13(16)
C(7)–N(1)–C(8)	114.5(5)	113.7(3)	113.8(3)
C(7)–N(1)–C(9)	121.9(4)	121.8(3)	123.0(3)
C(8)–N(1)–C(9)	121.2(4)	119.9(2)	120.7(3)

Although the bond lengths in the structures **7–9** are remarkably similar to those of **7s–9s**, it is noteworthy that the Fe–Fe bond lengths are elongated to 2.5475(10) Å for **7**, 2.5572(5) Å for **8**, 2.5514(9) Å for **9**, which are larger than those of **7s–9s** (2.4998(10) Å for **7s**, 2.5047(6) Å for **8s** and 2.5090(10) Å for **9s**)[9a,c,13c] and other reported hexa-carbonyl aza dithiolate diiron derivatives (2.49–2.51 Å).[9,24] The Fe–Fe bond lengths of **7–9** are much close to the corresponding ones in the reduced form (2.55 Å),[5] although a little shorter than those in the oxidized form (*ca.* 2.60 Å)[4a,b] of the metalloenzymes in the micro-biosystem. The recent research revealed that the more electron rich is in the iron core, the longer the Fe–Fe bond is.[25] However, the average ν(CO) values indicate that the electron density at the iron cores of **7–9** is slight higher than those of **7s–9s**. Thus, the steric influence of the relatively bulky Se atoms may primarily lengthen the Fe-Fe distances for **7–9**.

There is a simple packing and no hydrogen bonds and no π–π stacking interactions in the crystal cell packing graphs of complexes **7–9**. The van der Waals forces are primarily responsible for the interactions between molecules, which is similar to those of **7s–9s**.[9a,c,13c]

Cyclic voltammograms of complexes 7–9

The iron core plays an important role in the process of H_2 production. Thus, the redox properties of the iron cores of

Table 3 Redox potentials of complexes **7–9** and their dithiolate analogous **7s–9s**[a]

Complex	E_{pa}/V ($Fe^{I}Fe^{I}/Fe^{I}Fe^{II}$)	E_{pa}/V ($Fe^{I}Fe^{II}/Fe^{II}Fe^{II}$)	E_{pc}/V ($Fe^{I}Fe^{I}/Fe^{I}Fe^{0}$)	E_{pc}/V ($Fe^{I}Fe^{0}/Fe^{0}Fe^{0}$)
7	0.66		−1.40	−1.71
8	0.58	0.84	−1.49	−2.02
9	0.57	0.89	−1.50	−2.00
7s	0.76		−1.41	−1.76
8s	0.64		−1.50	−1.99
9s	0.64		−1.50	−1.99

[a] 0.05 M n-Bu_4NPF_6 in CH_3CN; scan rate: 100 mV s^{-1}. All potentials were measured under the same conditions using a non-aqueous $Ag/AgNO_3$ electrode as reference.

complexes **7–9** were investigated by cyclic voltammograms (CVs). To further understand these electrochemical characters, the CVs of complexes **7s–9s** were measured under the same conditions. All the CV measurements were carried out in CH_3CN solution. They were initiated from the open circuit and proceeded in the cathodic direction. While Table 3 lists the electrochemical data of **7–9** and **7s–9s**, Fig. 3 shows their cyclic voltammograms.

It has been demonstrated that **7** displayed two quasi-reversible reduction and one irreversible oxidation events, while **8** and **9** manifested one quasi-reversible, one irreversible reduction and two irreversible oxidation events. The defined waves are actually similar to the typical ones of the ADT-bridged dithiolate series.[9b,c,13c,24] The first and second reduction events of **7** (−1.40, −1.71 V), **8** (−1.49, −2.02 V) and **9** (−1.50, −2.00 V) (*vs.* Ag/Ag^+, 0.01 M $AgNO_3$) could be assigned to the one-electron reduction processes of $Fe^{I}Fe^{I}$ to $Fe^{I}Fe^{0}$ and $Fe^{I}Fe^{0}$ to $Fe^{0}Fe^{0}$. Similarly, the first oxidation events at 0.66 V for **7**, 0.58 V for **8** and 0.57 V for **9** should be attributed to the one-electron oxidation processes of $Fe^{I}Fe^{I}$ to $Fe^{I}Fe^{II}$, while the second oxidation events for **8** at 0.84 V and **9** at 0.89 V were ascribed to the second electron-transfer processes of $Fe^{I}Fe^{II}$ to $Fe^{II}Fe^{II}$. Noticeably, it could be seen that the $Fe^{I}Fe^{I}/Fe^{I}Fe^{II}$ oxidation events of **7–9** are apparently shifted towards less positive potentials (ΔE = 70–100 mV) than the corresponding oxidation events of **7s–9s** (0.76 V for **7s**, 0.64 V for **8s** and **9s**). Meanwhile, no $Fe^{I}Fe^{II}/Fe^{II}Fe^{II}$ oxidation events for **8s** and **9s** were observed within the electrochemical window of solvent. These electrochemical behaviors demonstrate that complexes **7–9** are somewhat easier to oxidize and convey the same message, as shown by the ν(CO) values of IR data, that the average electron density of iron cores of **7–9** is slightly higher than those of **7s–9s**.

Compared with **7**, complexes **8** and **9** could be easier to oxidize and more difficult to reduce. These observations indicated that the strong inductive effect of the p-substituted NO_2 group may decrease the electron density in the π system of the phenyl ring attaching to the bridged N atom, and slightly decrease the electron accumulation on the iron core through the three atoms (N, C, Se), resulting in the less negative reduction and more positive oxidation potentials for complex **7** as compared to **8** and **9**.

Interestingly, although the more negative $Fe^{I}Fe^{I}/Fe^{I}Fe^{II}$ oxidation potentials and the higher average ν(CO) values of **7–9** compared to those of **7s–9s** suggest that the average electron density of iron cores in **7–9** is higher than that in **7s–9s** as described above, the first $Fe^{I}Fe^{I}/Fe^{I}Fe^{0}$ and the second $Fe^{I}Fe^{0}/Fe^{0}Fe^{0}$ reduction potentials of **7–9** (−1.40 and −1.71 V for **7**, −1.49 and −2.02 V for **8** and −1.50 and −2.00 V for **9**) are roughly the same relative to the corresponding ones of **7s–9s** (−1.41 and −1.76 V for **7s**, −1.50 and −1.99 V for **8s** and **9s**). The enhancement of the electron accumulations on the iron cores by changing the coordinating S atoms of the bridging ligands to Se atoms dose not result in the cathodic shifts for the reduction potentials of the iron cores and it features the diselenide diiron complexes. Whereas, further work is needed to elucidate this aspect of the electrochemistry.

Electrocatalytic proton reduction by complex 9

To avoid the influence of the NO_2 group on the cyclic voltammograms, complexes **8** and **9** were chosen to investigate the electrocatalytic proton reduction in the presence of HOTs (0–9 mM). As complexes **8** and **9** display similar electrochemical behaviors at variant acid concentrations, herein we reported the

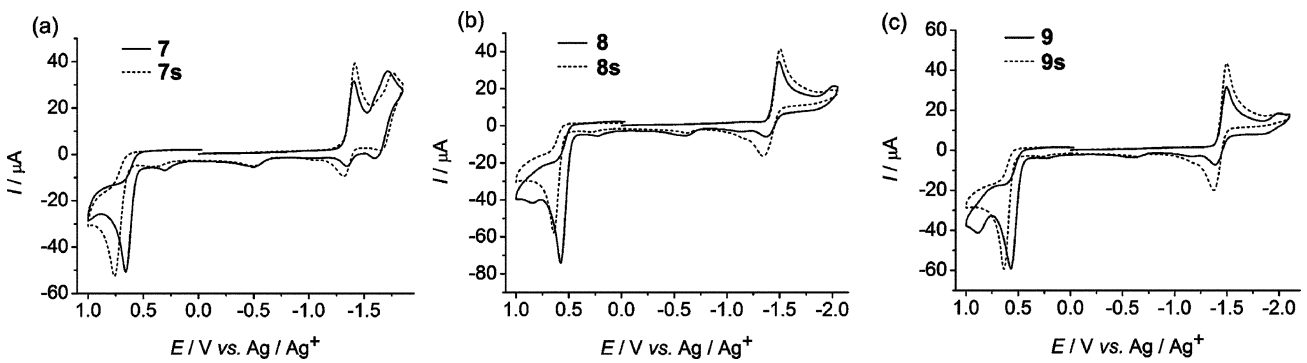

Fig. 3 Cyclic voltammograms of complexes **7** and **7s** (a), **8** and **8s** (b), and **9** and **9s** (c), 1.0 mM in 0.05 M n-Bu_4NPF_6/CH_3CN solution at a potential scan rate of 100 mV s^{-1}.

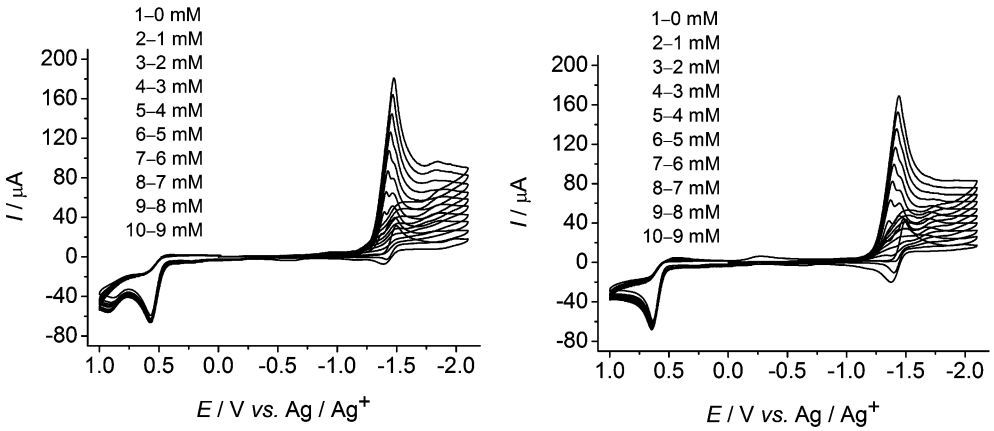

Fig. 4 Cyclic voltammograms of complexes **9** (left) and **9s** (right) with 1.0 mM complex and 0–9 mM HOTs in 0.05 M n-Bu_4NPF_6–CH_3CN solution at a potential scan rate of 100 mV s^{-1}.

cyclic voltammograms of **9** together with **9s** under the same acid conditions for a direct comparison of the electrocatalytic activity (Fig. 4).

Upon addition of 1 mM of HOTs, new reduction events were observed at −1.37 V for **9** and −1.34 V for **9s**. These events were more positive than those of the initial Fe^IFe^I/Fe^IFe^0 reduction processes and indicated the catalytic proton reduction.[7d] The second reduction events still corresponded to the one-electron Fe^IFe^I/Fe^IFe^0 reduction processes of **9** and **9s**. The current intensity of the first reduction events at −1.37 V for **9** and −1.34 V for **9s** show a significant electrocatalytic response and gradually increase with increasing acid concentration, while their potentials shift towards a relatively more negative potential. All these electrochemical behaviors feature an electrocatalytic proton reduction process.[7d,h,i,9b,c,15b,26]

Fig. 5 presents plots of current intensity of the electrocatalytic events *vs.* acid concentration of HOTs in CH_3CN for **9** and **9s**. The current intensity of the electrocatalytic events of **9** and **9s** both display a good linear increase with sequential increase of the concentration of HOTs. The steeper slopes displayed by complex **9** are indicative of slightly greater sensitivity of the reduced species to acid concentration, as compared to that exhibited by **9s** under the same measuring conditions. That is, complex **9** displayed a relatively high electrocatalytic activity for reduction of protons from HOTs, even though the electrocatalytic event potential is

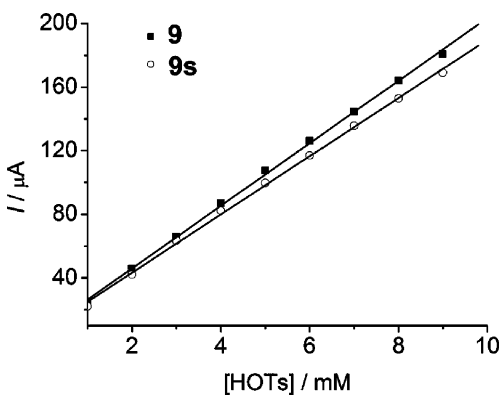

Fig. 5 Dependence of current heights of electrocatalytic events on the concentration of HOTs in CH_3CN for complexes **9** and **9s**.

roughly the same as **9s** (−1.37 V for **9** and −1.34 V for **9s**). The slightly higher electron density of iron core of **9** presumably makes the reduced intermediates more stable and results in a relatively high electrocatalytic activity of **9** as compared to **9s**. Our results indicate the affirmative effects of changing the coordinating S atoms of the bridging ligands to Se atoms on the electrocatalytic activity of model complexes and may provide us an insight into designing new types of diselenide diiron model complexes.

Conclusions

Three selenium-bridged diiron hexa-carbonyl complexes $[\{(\mu\text{-}SeCH_2)_2NC_6H_4R\}Fe_2(CO)_6]$ (R = 4-NO_2, **7**; R = H, **8**; R = 4-CH_3, **9**) were firstly synthesized and well characterized as models for the active site of Fe–Fe hydrogenases. As expected, the overall molecular geometries of **7–9** are analogous to those of their dithiolate analogues $[\{(\mu\text{-}SCH_2)_2NC_6H_4R\}Fe_2(CO)_6]$ (R = 4-NO_2, **7s**; R = H, **8s**; R = 4-CH_3, **9s**). The IR spectra indicate that changing the coordinating S atoms of the bridging ligands to Se atoms enhances the average electron density of the iron cores for complexes **7–9**. This affect is also consistent with the evidences: (i) the shift of the Fe^IFe^I/Fe^IFe^{II} oxidation potentials of **7–9** to less positive values; (ii) the appearance of the $Fe^IFe^{II}/Fe^{II}Fe^{II}$ oxidation events for **8** and **9**. However, the Fe^IFe^I/Fe^IFe^0 and Fe^IFe^0/Fe^0Fe^0 reduction potentials of **7–9** are roughly the same as those of **7s**–**9s**. As a typical object we chose, complex **9** has a slightly higher electrocatalytic activity for reduction of protons from HOTs than its dithiolate analogue **9s**. These electrochemical observations are particular and may indicate the better capability of catalyzing electrochemical reduction of proton for the selenium-bridged diiron complexes. To obtain more efficient proton reduction electrocatalysts and further understand the electrochemical behaviors of such selenium-bridged system, structural modifications of complexes **7–9** with good donor ligands are now in progress.

Experimental

Reagents and instruments

All reactions and operations related to organometallic complexes were carried out under a dry, prepurified nitrogen atmosphere with standard Schlenk techniques. All solvents were dried and distilled

prior to use according to standard methods. Paraformaldehyde, 4-nitroaniline, aniline, 4-methylaniline and $[Fe(CO)_5]$ were available commercially and used without further purification. The reagents $LiEt_3BH$ and CF_3COOH were purchased from Aldrich. The starting complexes *N*,*N*-bis(hydroxymethyl)-4-nitroaniline (**1**), *N*,*N*-bis(hydroxymethyl)aniline (**2**), *N*,*N*-bis(hydroxymethyl)-4-methylaniline (**3**) and $[(\mu\text{-Se})_2Fe_2(CO)_6]$ (**4**) were prepared according to the literature methods.[18–20] Three dithiolate analogues $[\{(\mu\text{-SCH}_2)_2N(4\text{-NO}_2C_6H_4)\}Fe_2(CO)_6]$ (**7s**), $[\{(\mu\text{-SCH}_2)_2NC_6H_5\}Fe_2(CO)_6]$ (**8s**) and $[\{(\mu\text{-SCH}_2)_2N(4\text{-CH}_3C_6H_4)\}Fe_2(CO)_6]$ (**9s**) were generated following the published procedures.[9a,c,13c] IR spectra were recorded on JASCO FT/IR 430 spectrophotometer. ^1H and ^{13}C NMR spectra were collected on a Varian Inova 400 NMR spectrometer with tetramethylsilane (TMS) as internal standard. HR-MS spectra determinations were made on a GCT-MS instrument (Micromass, England).

Preparation of $[\{(\mu\text{-SeCH}_2)_2N(4\text{-NO}_2C_6H_4)\}Fe_2(CO)_6]$ (7)

$LiEt_3BH$ solution (1 M solution in THF, 2.3 mL, 2.3 mmol) was added to a fresh prepared solution of $[(\mu\text{-Se})_2Fe_2(CO)_6]$ (**4**) (0.5 g, 1.15 mmol) in THF (20 mL) by syringe at −78 °C over 20 min. The mixture was stirred for 1 h at −78 °C and the color of the solution turned from red–purple to dark red–brown. The resulting lithium salt $[(\mu\text{-LiSe})_2Fe_2(CO)_6]$ (**5**) solution was treated dropwise with CF_3COOH (0.17 mL, 2.3 mmol) to give $[(\mu\text{-HSe})_2Fe_2(CO)_6]$ (**6**). A solution of **1** (0.912 g, 4.6 mmol), prepared from 4-nitroaniline and paraformaldehyde, in THF (10 mL) was added to the THF solution of **6**. After the mixture was warmed to room temperature and continually stirred for 5 h, the solvent was removed on a rotary evaporator to give a dark-brown solid. The crude product was purified by column chromatography on silica gel using CH_2Cl_2–hexane (1 : 2) as eluent to give complex **7** as a dark purple solid (0.319 g, 46%). Recrystallization in the CH_2Cl_2/pentane solution afforded crystals of **7** suitable for X-ray study. ^1H NMR ($CDCl_3$): δ 8.234 (d, 2H), 6.825 (d, 2H), 4.594 (s, 4H) ppm; ^{13}C NMR ($CDCl_3$): δ 207.50, 147.96, 140.43, 126.71, 114.52, 42.12 ppm; IR (CH_2Cl_2): ν_{max}/cm^{-1} 2070, 2033, 1999 (CO); HR-MS (EI): *m*/*z* calc. for $[M^+]$: 603.7310; found: 603.7305.

Preparation of $[\{(\mu\text{-SeCH}_2)_2NC_6H_5\}Fe_2(CO)_6]$ (8)

The similar procedure was followed as for **7**, but 0.705 g (4.6 mmol) of **2**, prepared from aniline and paraformaldehyde, was employed instead of **1**. After purified by column chromatography on silica gel using CH_2Cl_2–hexane (1 : 10) as eluent, 0.334 g (52%) of **8** was obtained as a dark purple solid. Crystals suitable for X-ray study were grown from a mixed CH_2Cl_2–pentane solution. ^1H NMR ($CDCl_3$): δ 7.341 (t, 2H), 6.996 (t, 1H), 6.834 (d, 2H), 4.540 (s, 4H) ppm; ^{13}C NMR (100 MHz, $CDCl_3$): δ 207.76, 142.91, 130.40, 120.66, 115.56, 43.86 ppm; IR (CH_2Cl_2): ν_{max}/cm^{-1} 2067, 2030, 1994 (CO); HR-MS (EI) : *m*/*z* calc. for $[M^+]$: 558.7459; found: 558.7462.

Preparation of $[\{(\mu\text{-SeCH}_2)_2N(4\text{-CH}_3C_6H_4)\}Fe_2(CO)_6]$ (9)

The similar procedure was followed as for **7**, but 0.769 g (4.6 mmol) of **2**, prepared from 4-methylaniline and paraformaldehyde, was employed in place of **1**. After purified by column chromatography on silica gel using CH_2Cl_2–hexane (1 : 10) as eluent, 0.323 g (49%) of **9** was obtained as a dark purple solid. Crystals suitable for X-ray study were grown from a mixed CH_2Cl_2–pentane solution. ^1H NMR ($CDCl_3$): δ 7.139 (d, 2H), 6.728 (d, 2H), 4.530 (s, 4H), 2.256

Table 4 Crystallographic data and structural refinement parameters for **7–9**

	7	**8**	**9**
Empirical formula	$C_{14}H_8Fe_2N_2O_8Se_2$	$C_{14}H_9Fe_2NO_6Se_2$	$C_{15}H_{11}Fe_2NO_6Se_2$
M_r	601.84	556.84	570.87
Crystal system	Monoclinic	Monoclinic	Triclinic
Space group	$P2_1$	$P2_1/n$	$P\bar{1}$
a/Å	7.7173(3)	8.0764(6)	7.835(2)
b/Å	10.5330(4)	12.3471(8)	9.930(3)
c/Å	11.9968(4)	17.7225(12)	12.436(3)
α/°	90.00	90.00	100.133(3)
β/°	104.189(2)	91.866(4)	101.395(3)
γ/°	90.00	90.00	90.643(3)
V/Å^3	945.43(6)	1766.4(2)	932.6(4)
Z	2	4	2
D_c/g cm^{-3}	2.114	2.094	2.033
μ/mm^{-1}	5.429	5.793	5.489
F(000)	580	1072	552
Flack parameter	0.018(9)	—	—
Crystal size/mm	0.20 × 0.10 × 0.02	0.33 × 0.26 × 0.15	0.43 × 0.05 × 0.05
$\theta_{min/max}$/°	1.75–27.49	2.01–28.00	2.09–29.17
Reflections collected	12039	22004	5855
Independent reflections	4072	4270	4317
R_{int}	0.0472	0.0370	0.0193
Parameters refined	253	227	235
GOF on F^2	0.960	1.058	0.993
R_1,[a] wR_2[b] [$I > 2\sigma(I)$]	0.0344, 0.0493	0.0255, 0.0569	0.0368, 0.0784
R_1,[a] wR_2[b] (all data)	0.0557, 0.0551	0.0356, 0.0596	0.0601, 0.0876
$\Delta\rho_{max/min}$/e Å^{-3}	0.385/–0.366	0.919/–0.837	0.551/–0.472

[a] $R_1 = \sum\|F_o\| - |F_c\|$. [b] $wR_2 = [\sum[w(F_o^2 - F_c^2)^2]/\sum w(F_o^2)^2]^{1/2}$.

(s, 3H) ppm; ^{13}C NMR ($CDCl_3$): δ 207.53, 140.55, 130.89, 130.18, 115.59, 44.29, 20.67 ppm; IR (CH_2Cl_2): ν_{max}/cm^{-1} = 2064, 2023, 1983 (CO); HR-MS (EI) : m/z calc. for [M$^+$]: 572.7616; found: 572.7614.

X-Ray crystal structure determination of complexes 7–9

Diffraction measurements of **7–9** were made on a SMART APEX II diffractometer. Data were collected at 298 K using graphite-monochromated Mo-Kα radiation (λ = 0.71073 Å) in the ω–2θ scan mode. Data processing was accomplished with the SAINT processing program.[27] Intensity data were corrected for absorption by the SADABS program.[28] The structures were solved by direct methods and refined by full-matrix least-squares techniques on F_o^2 using the SHELXTL 97 crystallographic software package.[29] All non-hydrogen atoms were refined anisotropically. All hydrogen atoms were located by using the geometric method, and their positions and thermal parameters were fixed during the structure refinement. Details of crystal data, data collections, and structure refinements are summarized in Table 4.

CCDC reference numbers 665465 for **7**, 665466 for **8** and 665467 for **9**.

For crystallographic data in CIF or other electronic format see DOI: 10.1039/b717497g

Electrochemistry studies of complexes 7–9

The acetonitrile (Aldrich, spectroscopy grade) used for electrochemical measurements was dried with molecular sieves and then freshly distilled from CaH_2 under N_2. A solution of 0.05 M n-Bu_4NPF_6 (Fluka, electrochemical grade) in CH_3CN was used as electrolyte in all cyclic voltammetric experiments. The supporting electrolyte solution was degassed by bubbling with dry argon for 10 min before measurement. Electrochemical measurements were made with a BAS 100B electrochemical workstation at a scan rate of 100 mV s^{-1}. All voltammograms were obtained in a conventional three-electrode cell under argon and at ambient temperature. The working electrode was a glassy carbon disc (diameter 3 mm) that was successively polished with 3-μm and 1-μm diamond pastes and sonicated in ion-free water for 15 min prior to use. The experimental reference electrode was a non-aqueous Ag/Ag$^+$ electrode (0.01 M $AgNO_3$–0.1 M n-Bu_4NPF_6 in CH_3CN) and the counter electrode was a platinum wire.

Acknowledgements

We are grateful to the National Natural Science Foundation of China (Projects 20725621 and 20706008) and the Cultivation Fund of the Key Scientific and Technical Innovation Project, Ministry of Education of China (707016) for financial support of this work. Helpful discussions with Dr. Ping Li are gratefully acknowledged.

References

1 (*a*) M. W. W. Adams and E. I. Stiefel, *Science*, 1998, **282**, 1842–1843; (*b*) R. Cammack, *Nature*, 1999, **397**, 214–215; (*c*) M. Y. Darensbourg, E. J. Lyon and J. J. Smee, *Coord. Chem. Rev.*, 2000, **206–207**, 533–561; (*d*) M. Y. Darensbourg, E. J. Lyon, X. Zhao and I. P. Georgakaki, *Proc. Natl. Acad. Sci. U. S. A.*, 2003, **100**, 3683–3688; (*e*) X. Liu, S. K. Ibrahim, C. Tard and C. J. Pickett, *Coord. Chem. Rev.*, 2005, **249**, 1641–1652.

2 M. W. W. Adams, *Biochim. Biophys. Acta*, 1990, **1020**, 115–145.

3 M. Frey, *ChemBioChem*, 2002, **3**, 153–160.

4 (*a*) J. W. Peters, W. N. Lanzilotta, B. J. Lemon and L. C. Seefeldt, *Science*, 1998, **282**, 1853–1858; (*b*) Y. Nicolet, C. Piras, P. Legrand, E. C. Hatchikian and J. C. Fontecilla-Camps, *Structure*, 1999, **7**, 13–23; (*c*) Z. Chen, B. J. Lemon, S. Huang, D. J. Swartz, J. W. Peters and K. A. Bagley, *Biochemistry*, 2002, **41**, 2036–2043; (*d*) A. L. De Lacey, C. Stadler, C. Cavazza, E. C. Hatchikian and V. M. Fernandez, *J. Am. Chem. Soc.*, 2000, **122**, 11232–11233.

5 Y. Nicolet, A. L. Lacey, X. Vernéde, V. M. Fernandez, E. C. Hatchikian and J. C. Fontecilla-Camps, *J. Am. Chem. Soc.*, 2001, **123**, 1596–1601.

6 H. J. Han and M. B. Hall, *J. Am. Chem. Soc.*, 2001, **123**, 3828–3829.

7 (*a*) M. Schmidt, S. M. Contakes and T. B. Rauchfuss, *J. Am. Chem. Soc.*, 1999, **121**, 9736–9737; (*b*) E. J. Lyon, I. P. Georgakaki, J. H. Reibenspies and M. Y. Darensbourg, *J. Am. Chem. Soc.*, 2001, **123**, 3268–3278; (*c*) F. Gloaguen, J. D. Lawrence, M. Schmidt, S. R. Wilson and T. B. Rauchfuss, *J. Am. Chem. Soc.*, 2001, **123**, 12518–12527; (*d*) F. Gloaguen, J. D. Lawrence and T. B. Rauchfuss, *J. Am. Chem. Soc.*, 2001, **123**, 9476–9477; (*e*) F. Gloaguen, J. D. Lawrence, T. B. Rauchfuss, M. Bénard and M. M. Rohmer, *Inorg. Chem.*, 2002, **41**, 6573–6582; (*f*) X. Zhao, I. P. Georgakaki, M. L. Miller, J. C. Yarbrough and M. Y. Darensbourg, *J. Am. Chem. Soc.*, 2001, **123**, 9710–9711; (*g*) X. Zhao, I. P. Georgakaki, M. L. Miller, R. Mejia-Rodriguez, C. Y. Chiang and M. Y. Darensbourg, *Inorg. Chem.*, 2002, **14**, 3917–3928; (*h*) D. Chong, I. P. Georgakaki, R. Mejia-Rodriguez, J. Sanabria-Chinchilla, M. P. Soriaga and M. Y. Darensbourg, *Dalton Trans.*, 2003, 4158–4163; (*i*) R. Mejia-Rodriguez, D. Chong, J. H. Reibenspies, M. P. Soriaga and M. Y. Darensbourg, *J. Am. Chem. Soc.*, 2004, **126**, 12004–12014.

8 (*a*) S. J. George, C. Cui, M. Razavet and C. J. Pickett, *Chem.–Eur. J.*, 2002, **8**, 4037–4046; (*b*) M. Razavet, S. C. Davies, D. L. Hughes, J. E. Barclay, D. J. Evans, S. A. Fairhurst, X. Liu and C. J. Pickett, *Dalton Trans.*, 2003, 586–595; (*c*) D. J. Evans and C. J. Pickett, *Chem. Soc. Rev.*, 2003, **32**, 268–275; (*d*) C. Tard, X. Liu, S. K. Ibrahim, M. Bruschi, L. D. Glola, S. C. Davies, X. Yang, L. Wang, G. Sawers and C. J. Pickett, *Nature*, 2005, **433**, 610–613.

9 (*a*) H. Li and T. B. Rauchfuss, *J. Am. Chem. Soc.*, 2002, **104**, 726–727; (*b*) S. Ott, M. Kritikos, B. Åkermark, L. Sun and R. Lomoth, *Angew. Chem., Int. Ed.*, 2004, **43**, 1006–1009; (*c*) T. Liu, M. Wang, Z. Shi, H. Cui, W. Dong, J. Chen, B. Åkermark and L. Sun, *Chem.–Eur. J.*, 2004, **10**, 4474–4479; (*d*) F. Wang, M. Wang, X. Liu, K. Jin, W. Dong, G. Li, B. Åkermark and L. Sun, *Chem. Commun.*, 2005, 3221–3223; (*e*) L. Song, M. Tang, F. Su and Q. Hu, *Angew. Chem., Int. Ed.*, 2006, **45**, 1130–1133.

10 (*a*) J. D. Lawrence, H. Li and T. B. Rauchfuss, *Chem. Commun.*, 2001, 1482–1483; (*b*) J. D. Lawrence, H. Li, T. B. Rauchfuss, M. Bénard and M. M. Rohmer, *Angew. Chem., Int. Ed.*, 2001, **40**, 1768–1771; (*c*) S. Ott, M. Borgström, M. Kritikos, R. Lomoth, J. Bergquist, B. Åkermark, L. Hammarström and L. Sun, *Inorg. Chem.*, 2004, **43**, 4683–4692.

11 (*a*) P. Li, M. Wang, C. He, G. Li, X. Liu, C. Chen, B. Åkermark and L. Sun, *Eur. J. Inorg. Chem.*, 2005, 2506–2513; (*b*) W. Dong, M. Wang, X. Liu, K. Jin, G. Li, F. Wang and L. Sun, *Chem. Commun.*, 2006, 305–307; (*c*) L. Schwartz, G. Eilers, L. Eriksson, A. Gogoll, R. Lomoth and S. Ott, *Chem. Commun.*, 2006, 520–522; (*d*) J. Hou, X. Peng, Z. Zhou, S. Sun, X. Zhao and S. Gao, *J. Organomet. Chem.*, 2006, **691**, 4633–4640; (*e*) P. Li, M. Wang, C. He, G. Li, X. Liu, K. Jin and L. Sun, *Eur. J. Inorg. Chem.*, 2007, 3718–3727.

12 A. Le Cloirec, S. P. Best, S. Borg, S. C. Davies, D. J. Evana, D. L. Hughes and C. J. Pickett, *Chem. Commun.*, 1999, 2285–2286.

13 (*a*) J. L. Nehring and D. M. Heinekey, *Inorg. Chem.*, 2003, **42**, 4288–4292; (*b*) C. A. Boyke, T. B. Rauchfuss, S. R. Wilson, M. M. Rohmer and M. Bénard, *J. Am. Chem. Soc.*, 2004, **126**, 15151–15160; (*c*) J. Hou, X. Peng, J. Liu, Y. Gao, X. Zhao, S. Gao and K. Han, *Eur. J. Inorg. Chem.*, 2006, 4679–4686.

14 (*a*) J. F. Capon, S. E. Hassnaoui, F. Gloaguen, P. Schollhammer and J. Talarmin, *Organometallics*, 2005, **24**, 2020–2022; (*b*) J. W. Tye, J. Lee, H. W. Wang, R. Mejia-Rodriguez, J. H. Reibenspies, M. B. Hall and M. Y. Darensbourg, *Inorg. Chem.*, 2005, **44**, 5550–5552; (*c*) L. Duan, M. Wang, P. Li, Y. Na, N. Wang and L. Sun, *Dalton Trans.*, 2007, 1277–1283; (*d*) D. Morvan, J. F. Capon, F. Gloaguen, A. L. Goff, M. Marchivie, F. Michaud, P. Schollhammer, J. Talarmin and J. J. Yaouanc, *Organometallics*, 2007, **26**, 2042–2052.

15 (*a*) L. Song, Z. Yang, H. Bian and Q. Hu, *Organometallics*, 2004, **23**, 3082–3084; (*b*) L. Song, Z. Yang, H. Bian, Y. Liu, H. Wang, X. Liu and Q. Hu, *Organometallics*, 2005, **24**, 6126–6135; (*c*) L. Song, Z. Yang, Y. Hua, H. Wang, Y. Liu and Q. Hu, *Organometallics*, 2007,

26, 2106–2110; (*d*) J. Windhager, M. Rudolph, S. Bräutigam, H. Görls and W. Weigand, *Eur. J. Inorg. Chem.*, 2007, 2748–2760.
16 M. H. Cheah, S. J. Borg, M. I. Bondin and S. P. Best, *Inorg. Chem.*, 2004, **43**, 5635–5644.
17 P. Das, J. F. Capon, F. Gloaguen, F. Y. Pétillon, P. Schollhammer, J. Talarmin and K. W. Muir, *Inorg. Chem.*, 2004, **43**, 8203–8205.
18 H. Hongo, K. Iwasa, C. Kabuto, H. Matsuzaki and H. Nakano, *J. Chem. Soc., Perkin Trans. 1*, 1997, 1747–1754.
19 D. Seyferth and R. S. Henderson, *J. Organomet. Chem.*, 1981, **204**, 333–343.
20 P. Mathur, D. Chakrabarty, M. M. Hassain, R. S. Rashid, V. Rugmini and A. L. Pheingold, *Inorg. Chem.*, 1992, **31**, 1106–1108.
21 C. F. Campana, F. Yip-Kwailo and L. F. Dahl, *Inorg. Chem.*, 1979, **18**, 3060–3064.
22 J. A. Gladysz, J. L. Hornby and J. E. Garbe, *J. Org. Chem.*, 1978, **43**, 1204–1208.
23 R. Rossetti, G. Gervasio and P. L. Stanghellini, *Inorg. Chim. Acta*, 1979, **35**, 73–78.
24 (*a*) L. Song, J. Ge, X. Zhang, Y. Liu and Q. Hu, *Eur. J. Inorg. Chem.*, 2006, 3204–3210; (*b*) L. Song, J. Ge, X. Liu, L. Zhao and Q. Hu, *J. Organomet. Chem.*, 2006, **691**, 5701–5709; (*c*) S. Jiang, J. Liu, Y. Shi, Z. Wang, B. Åkermark and L. Sun, *Dalton Trans.*, 2007, 896–902.
25 Y. Si, C. Ma, M. Hu, H. Chen, C. Chen and Q. Liu, *New J. Chem.*, 2007, **31**, 1448–1454.
26 I. Bhugun, D. Lexa and J. M. Saveant, *J. Am. Chem. Soc.*, 1996, **118**, 3982–3983.
27 *Software packages SMART and SAINT*, Siemens Energy & Automation Inc., Madison, WI, 1996.
28 G. M. Sheldrick, *SADABS Absorption Correction Program*, University of Göttingen, Germany, 1996.
29 G. M. Sheldrick, *SHELXTL 97 Program for the Refinement of Crystal Structure*, University of Göttingen, Germany, 1997.